# SUPPLEMENTARY INFORMATION FOR:

# Stabilizing Leaflet Asymmetry under Differential Stress in a Highly Coarse-Grained Lipid Membrane Model

Samuel Foley and Markus Deserno*
*Department of Physics, Carnegie Mellon University, Pittsburgh, PA 15213, USA*
(Dated: August 9, 2022)

Here we present brief explanations of how observables were calculated from simulations.

### A. Area per lipid

The area per lipid $a_\ell$ is determined by simulating small bilayer patches of 128 lipids under conditions of zero tension and measuring the average projected area (*i.e.*, box size). Area measurements are done on small systems like this in order to avoid the effect of large membrane undulations contributing to a difference between frame area and total membrane area.

### B. Gel Transition Temperature

To determine the approximate location of the fluid-gel transition temperature, initially two simulations were carried out in which the temperature was dynamically varied during simulation, either warming or cooling the system at a rate of $10^{-6}\,\varepsilon/k_\mathrm{B}\tau$. The area per lipid is a convenient reporter of the phase transition due to the abrupt $\sim 10\%$ change in area as the system either melts or gels. The warming simulation was started from a gel state and heated until a melting transition was observed. For the other, the reverse simulation was performed, starting from fluid and cooling until a gel transition was observed. The downside of this technique is that it exhibits fairly pronounced hysteresis.

To circumvent this problem, we carried out constant-temperature simulations at evenly spaced points within the region of hysteresis. These simulations were performed with 800 lipids in an anisotropic box of side lengths $L_x = 2L_y$ which is allowed to fluctuate only in the $x$-direction. These simulations tended to relax rapidly to either the fluid or gel state, except in the vicinity of the transition around $k_\mathrm{B}T \approx 1.322\,\varepsilon$. In these simulations it was seen that the membrane area fluctuated significantly as compared to neighboring temperatures. Figure SI 1 shows the traces of area per lipid versus time for a few of these simulations.

* deserno@andrew.cmu.edu

### C. Bending modulus

We determined the bending modulus using two different methods—an active and a passive one. The first (active) one is through the simulation of buckled membrane strips, as described in [1, 2]. However, in our analysis we also take into account the possibility of *curvature softening*, as empirically modeled in [3], because the curvatures arising during bucking of small membrane patches turn out to be high enough for this to be statistically observable even for fluid membranes. If $K$ is the membrane's local extrinsic curvature (the sum of its two principal curvatures [4]), the theory posits an empirically softened curvature energy density of the form

$$e(K) = \frac{\kappa}{\ell^2}\left[\sqrt{1+K^2\ell^2}-1\right] \tag{SI 1a}$$

$$= \frac{1}{2}\kappa K^2 - \frac{1}{8}(\kappa\ell^2)K^4 + \mathcal{O}(K^6)\,, \tag{SI 1b}$$

which amends the usual quadratic curvature energy $\frac{1}{2}\kappa K^2$ [5] by a negative (*i.e.*, softening) quartic term, while still being overall convex and bounded below. In this expression $\kappa$ is the bending modulus of the bilayer and $\ell$ is the curvature softening length scale, a material parameter. This yields a series expansion for the stress-strain relation given by [3]

$$\frac{F_x(\gamma;\{\kappa,\delta\})}{L_y} = \kappa\left(\frac{2\pi}{L}\right)^2\left[1+\frac{1}{2}(1-3\delta^2)\gamma + \frac{3}{32}(3-14\delta^2+31\delta^4)\gamma^2+\mathcal{O}(\gamma^3)\right]\,, \tag{SI 2}$$

where $\gamma = (L-L_x)/L$ is the dimensionless buckling strain and $\delta = 2\pi\ell/L$ is a dimensionless softening parameter. We amend this by a fluctuation correction in the stress-strain analysis as described in [2],

$$\delta F_x = -\frac{3k_\mathrm{B}T}{2L}\sum_{n=0}^{\infty} d_n\gamma^n\,, \tag{SI 3}$$

in which the coefficients $d_n = \frac{2}{3}[(n+2)b_n-(n+1)b_{n+1}]$ are defined in terms of the prefactors $b_n$ of the $\gamma^n$ terms in Eqn. (SI 2). We use buckles of 1342 lipids inside an elongated box of fixed width $L_y = 12\,\sigma$ and a length $L_x$ determined by $\gamma$ and the resting length $L$, which we measure first in a box with zero tension along $L_x$.

The second method is a classical fluctuation analysis of a flat membrane. We fit the height fluctuation spectrum

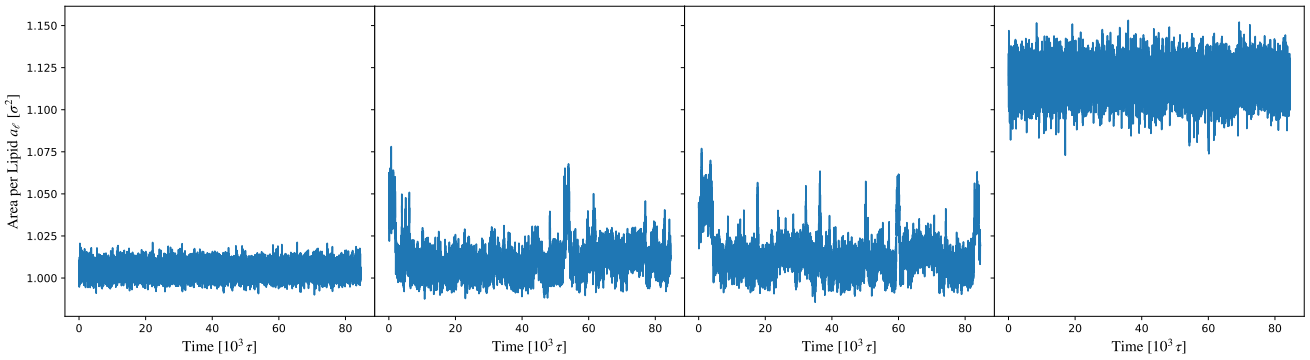


FIG. SI 1. Four traces of area per lipid in symmetric simulations of the four bead flip-fixed model at temperatures near $T_{\rm gel}$. From left to right the temperatures correspond to $k_{\rm B}T/\varepsilon$ =1.315, 1.32, 1.322, and 1.325.

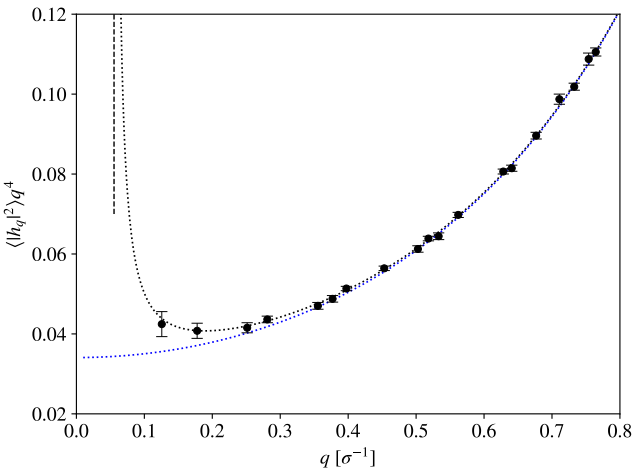


FIG. SI 2. Example of a fluctuation spectrum used to calculate $\kappa$, $\kappa_{\rm t,eff}$, and $q_{\rm c}$. Black dotted curve shows fit to Eqn. (SI 4) which includes a divergence at $q = \sqrt{-\Sigma/\kappa}$ due to a small residual compressive tension, with the dashed vertical segment indicating the asymptote. The blue dotted curve shows the fit to Eqn. (SI 4), except that $\Sigma$ is artificially set to zero after fitting, showing that the residual tension only affects the lowest few modes.

of our simulated membrane to the result of the theory by Terzi *et al.* [6, 7], amended by an additional tension:

$$\langle|h_q|^2\rangle = \frac{1}{1-(q/q_{\rm c})^2}\left[\frac{k_{\rm B}T}{\kappa q^4+\Sigma q^2}+\frac{k_{\rm B}T}{\kappa_{\rm t,eff}q^2}\right]. \quad \text{(SI 4)}$$

In this expression $q_{\rm c}$ is a critical wave vector of soft mode divergence, $\kappa$ is the bending modulus, $\Sigma$ is the lateral tension, and $\kappa_{\rm t,eff}$ is an effective lipid tilt modulus. We simulate 4316 lipids in a square membrane using a fixed side length of approximately $50\,\sigma$, determined by first finding the box size at which the membrane tension vanishes. 5000 equally spaced snapshots were collected along a trajectory of total length $100\,000\,\tau$, and errors in the fluctuation amplitudes were determined by blocking [8]. Figure SI 2 shows one such fluctuation spectrum along with the fit to Eqn. (SI 4). The maximum wave vector we fit to is $q_{\rm max} \approx 0.764\,\sigma^{-1}$. We used the set $\{\kappa, \kappa_{\rm t,eff}, q_{\rm c}\}$ as fitting parameters, but determined $\Sigma$ by measuring the (small) value of the lateral stress directly from the pressure tensor of the simulation box.

### D. Area expansion modulus

We find the area expansion modulus $K_A$ by simulating the same type of small patches used to measure $a_\ell$ (128 lipids—see Sec. A), but not just at zero tension. A range of fixed areas near the relaxed state are studied, and their lateral tension is measured as a function of area. Ignoring fluctuation corrections (which is legitimate for small patches), the elastic energy of stretching for such a situation is given by

$$E_A = \frac{1}{2}K_A A_0\left(\frac{A-A_0}{A_0}\right)^2. \quad \text{(SI 5)}$$

If $a = A/N$ is the area per lipid, and $a_\ell$ the resting area per lipid, then the mechanical tension $\Sigma$ in the membrane is given by

$$\Sigma(a) = \frac{\partial E_A}{\partial A} = K_A\left(\frac{a}{a_\ell}-1\right), \quad \text{(SI 6)}$$

an expression from which both $a_\ell$ and $K_A$ can be readily extracted.

### E. Orientational order parameter

The orientational ordering of the lipid molecules in the membrane is quantified by measuring the $P_2$ order parameter. If we consider a flat membrane in the $xy$-plane, then the orientation of each lipid has an instantaneous deflection $\theta$ away from the (average) membrane normal,

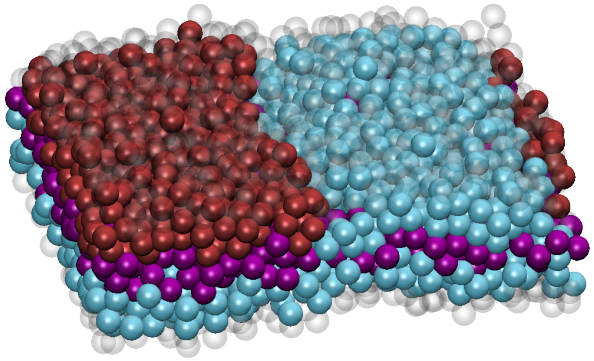

FIG. SI 3. Membrane simulation setup used to measure the line tension $\gamma$ which arises at the contact between unlike lipid domains in the flip-suppressed model. To distinguish the two different lipid types, the two middle beads of the different species are rendered as dark red and light blue. Head beads are drawn as colorless semi-transparent spheres, and final tail beads are dark purple. The total number of lipids is 800.

which here is just the $z$-direction. The $P_2$ order parameter essentially measures the degree of alignment implied by the underlying angular distribution function, and to account for the Jacobians of spherical symmetry, it is convenient to measure the ensemble average of the second Legendre polynomial of argument $\cos(\theta)$,

$$P_2 := \Big\langle \mathrm{P}_2\big(\cos(\theta)\big)\Big\rangle = \frac{1}{2}\big\langle 3\cos^2(\theta) - 1\big\rangle \ . \qquad \text{(SI 7)}$$

This takes on a value of 1 for a perfectly ordered system of crystalline lipids oriented normally to the bilayer plane, and a value of 0 for completely random orientations. We measure this in simulations of 800 lipids in a square membrane under conditions of zero tension.

### F. Line Tension between opposite leaflet lipids

In order to measure the line tension $\gamma$ produced at the contact line between two unlike lipid domains in the flip-suppressed model, we simulate a membrane as shown in Figure SI 3. The lower leaflet is entirely filled with one lipid type (say, the $\ominus$-type), while the upper leaflet contains an equal amount of $\oplus$- and $\ominus$-type lipids, arranged in two stripes as shown in the figure. The simulation box length is fixed in the direction parallel to the two contact lines, such that their length remains fixed. The box is allowed to fluctuate in the direction perpendicular to the lines to allow area equilibration at zero membrane tension. Observe that one leaflet has two unfavorable contact lines, while the other one has none, and so a state with an equal number of lipids on both sides need not be free of differential stress. However, half of the membrane area consists of a region where both the upper and the lower leaflet consist of $\ominus$-type lipids, and in that region lipid flip-flop is not suppressed, which permits a potential differential stress to relax.

The free energy of the system is lower for shorter contact lines, and therefore a tension arises in the direction parallel to these lines. If one writes the stress tensor for this system in Cartesian components where the $y$-axis is parallel to the lines, one finds

$$\sigma_{yy} = \frac{2\gamma}{L_x L_z}. \qquad \text{(SI 8)}$$

We therefore measure $\langle\sigma_{yy}\rangle$ in simulation using ESPResSo's volume-averaged stress tensor routine and use Eqn. (SI 8) to extract the value of $\gamma$.

### G. Diffusion Constant

Diffusion processes in two dimensions follow the relation

$$\big\langle [\boldsymbol{r}(t+\Delta t) - \boldsymbol{r}(t)]^2 \big\rangle = 4D\Delta t, \qquad \text{(SI 9)}$$

where $\boldsymbol{r}(t)$ is the position vector of a particle at time $t$, $\Delta t$ is the time difference over which we assess its diffusion, and $D$ is the diffusion constant. In our case, the system is not truly 2-dimensional, so $\boldsymbol{r}(t)$ is the projection of the lipid position vector onto the bilayer plane.

We take the average on the left side of Eqn. (SI 9) over each lipid in our membrane as well as over each pair of simulation configurations separated by $\Delta t$ in our output trajectory, with error bars computed by blocking [8]. By doing this calculation for 500 values of $\Delta t$ ranging from 100 $\tau$ to 20,000 $\tau$, we can fit the results to a line of slope $4D$ to determine the diffusion constant over this time interval. These calculations were performed on a system containing 2,000 lipids in a fixed-size square box with $L_x = L_y = 34.05\,\sigma$ simulated for 100,000 $\tau$.

### H. Bilayer Thickness

For our simple lipid models, we define the bilayer thickness as the mean difference in position perpendicular to the bilayer plane between the head beads of lipids in the upper and lower leaflets. These averages were performed on the same simulation trajectories used to measure the lipid orientational order parameter, containing 800 lipids and under conditions of zero bilayer tension.

[1] H. Noguchi, Anisotropic surface tension of buckled fluid membranes, Phys. Rev. E **83**, 061919 (2011).

[2] M. Hu, P. Diggins IV, and M. Deserno, Determining the bending modulus of a lipid membrane by simulating buck-

ling, The Journal of chemical physics **138**, 214110 (2013).
[3] P. Diggins IV, Z. A. McDargh, and M. Deserno, Curvature softening and negative compressibility of gel-phase lipid membranes, Journal of the American Chemical Society **137**, 12752 (2015).
[4] E. Kreyszig, *Differential Geometry*, 1st ed. (Dover, New York, 1991).
[5] W. Helfrich, Elastic properties of lipid bilayers: theory and possible experiments, Zeitschrift für Naturforschung C **28**, 693 (1973).
[6] M. M. Terzi and M. Deserno, Novel tilt-curvature coupling in lipid membranes, The Journal of Chemical Physics **147**, 084702 (2017).
[7] M. M. Terzi, M. F. Ergüder, and M. Deserno, A consistent quadratic curvature-tilt theory for fluid lipid membranes, The Journal of chemical physics **151**, 164108 (2019).
[8] H. Flyvbjerg and H. G. Petersen, Error estimates on averages of correlated data, J. Chem. Phys. **91**, 461 (1989).